Nigerian Journal of Physics (NJP)
ISSN online: 3027-0936
ISSN print: 1595-0611
DOI: https://doi.org/10.62292/njp.v35i1.2026.519
Volume 35(1), March 2026

Theoretical and Predictive Models of Particle Dynamics in Cassava Starch-Polyvinylpyrrolidone Nanocomposite Polymer Electrolytes for Lithium-Ion Batteries

***Iyamu O. Ceasar, Ewa I. Inuwa and Lumbi I. Williams**

Department of Physics, Nasarawa State University, Keffi, Nasarawa State, Nigeria.

*Corresponding Author's Email: caesariyamu71@gmail.com

ABSTRACT

Due to the growing demand for an eco-friendly lithium-ion battery sustainable energy storage system, this study investigated the theoretical and predictive models of particle dynamics in cassava starch (CS)-polyvinylpyrrolidone (PVP) nanocomposite polymer electrolytes for lithium-ion batteries. In this study, the material composition consists of CS and PVP in five different mass ratios, with the addition of fixed additives comprising glycerol, borax, TiO_2 and lithium acetate dihydrate. These materials were condensed into nanocomposite polymer electrolyte films using the direct-heating solution casting method. The data collected from these samples were analyzed using ionic conductivity, Nernst-Einstein, Fick's law of diffusion, Faraday's law of electrolysis, stress-strain, and Kissinger activation theoretical models; while, multiple regression model was employed as the predictive model. Results indicated that Sample 3 recorded the highest ionic conductivity (1.74×10^{-3} S/cm), highest ionic diffusion coefficient (3.34×10^{-9} cm^2/s), highest diffusion flux (2.31×10^{-4} mol/m^2.s) and highest electric charge (3.94×10^{-3} C/s). Tensile results showed that Sample 1 had the highest ultimate tensile strength (0.589 N/mm^2), and strain (55.25 %). Thermal analysis revealed that Sample 5 recorded the highest thermal stability(194 KJ/mol). Predictive model showed a strong predictive performance for activation energy ($R^2 = 0.97$). Overall, Sample 3 (2.5 g CS: 2.5 g PVP) demonstrated the best combination of electrochemical, tensile, and thermal properties for an eco-friendly lithium-ion battery application.

Keywords:
Nanocomposite polymer electrolyte,
Cassava starch biopolymer,
Polyvinylpyrrolidone synthetic polymer,
Theoretical Models,
Predictive Model.

INTRODUCTION

In the advancement of polymer electrolytes for energy storage systems- particularly lithium-ion batteries (LIB)- the role of particle dynamics in nanocomposite polymer electrolytes is of critical importance. In physics, the behavior of matter at the quantum scale -such as atoms, electrons, ions, and molecules- can be described in terms of its motions and interactions. These microscopic motions and interactions, collectively referred to as particle dynamics, influence the macroscopic performance of materials (Griffiths, 2008). In nanocomposite polymer electrolytes, quantum entities include polymer functional groups (hydroxyl and carbonyl), lithium salt species (Li^+), and nanoparticle constituents (Ti^{4+} and O^{2-}). Their motion involves translational motion and polymer segmental motion of polymer chains. These dynamic behavior at quantum level is often analyzed using theoretical models to predict the macroscopic performance of the electrolyte system, including ionic conductivity, tensile strength, and thermal stability (Cabaret *et.al.,* 2022; Patel, 2021).

Building on this understanding, at the microscopic level, the Li^+ in nanocomposite polymer electrolyte is what is responsible for the charging and discharging processes in LIBs. This charging-discharging cycles give LIBs a longer lifespan and faster charging capabilities compared to traditional batteries (Nagaura & Tozawa, 1990). As a result, they can be used in a variety of applications ranging from small electronics, such as smart phones and laptops, to large-scale systems, such as electric vehicles and renewable energy storage devices (Kittel, 2005). This electrical property defined by Li^+ transport, can be analyzed using theoretical models, including frequency-dependence response theory (Macdonald & Barsoukov, 2005), the Nernst-Einstein model (Armand & Tarascon, 2008), Fick's law of diffusion (Fong *et. al.,* 2021), and Faraday's law of electrolysis (Bard & Faulkner, 2021).

The tensile strength and thermal stability of nanocomposite polymer electrolytes are defined by polymer segmental chain motion and nanofiller interfacial motion of nanoparticles. The theoretical models used in the analysis of tensile strength and strain are stress-strain theory (Smith & Lee, 2021) and the rule of mixtures theory (Callister & Rethwisch, 2020), while the theoretical model used to analyze thermal stability is the Kissinger model (Song & Kwak, 2022), which is used to compute activation energy.

Most nanocomposite polymer electrolytes contain synthetic polymer, lithium salts, and additives, notably nanoparticles. The synthetic polymers in the system, contribute significantly to environmental challenges due to their toxic and non-biodegradable nature. Due to this problem, recent innovation is to include biopolymer either partially or wholly for the purpose of producing an ecofriendly environment (Wang *et. al.,* 2019). Raihan *et. al.* (2022) further emphasized that biopolymer materials are biodegradable, inexpensive, abundant, less toxic, and eco-friendly.

In energy storage systems, biopolymer materials such as cellulose and starch derivatives have recently emerged as alternatives to synthetic polymers because of the flexibility of their polymer chains (Pathak *et.al*., 2014). Research studies on cassava starch biopolymers, used either wholly or partially to replace synthetic polymers in nanocomposite polymer electrolytes, are relatively new compared to numerous studies on polymer electrolytes that utilize only synthetic polymers (Patra *et.al.,* 2024).

In this study, the objectives are to evaluate the electrochemical performance (ionic conductivity, ionic diffusion coefficient, diffusion flux, and electric charge), tensile strength (ultimate tensile strength, and strain), and thermal stability performance of CS-PVP nanocomposite polymer electrolytes using theoretical and predictive models, for the purpose of determining the overall best performing ecofriendly electrolyte. The need to investigate the composite blend of CS and PVP in nanocomposite polymer electrolytes arises from the goal of developing more sustainable, efficient, and cost-effective materials for energy storage applications. Consequently, this study evaluates the particle dynamics in nanocomposite polymer electrolytes using theoretical and predictive models for LIBs applications.

Theoretical and Predictive Models

The theoretical and predictive models of particle dynamics in nanocomposite polymer electrolytes consist of the following:

Theoretical Models

Ionic Conductivity Model

Ionic conductivity (Lasia, 2014) is expressed as:

$$\sigma = \frac{L}{Rb\,.\,A} \qquad (1)$$

where σ = ionic conductivity (S/cm)
L = film thickness (cm)
Rb = bulk resistance (Ω)
A = electrode-electrolyte contact area (cm^2)

Typical ionic conductivities of nanocomposite polymer electrolytes at room temperature range from $10^{-6} - 10^{-3}$s/cm (Ramesh & Arof, 2021).

Nernst-Einstein Model

Nernst-Einstein model relates ionic conductivity to diffusion coefficient (D) of mobile ion in an electrolyte (Barde & Deschamps, 2015). Nernst-Einstein equation (Maier, 2004) is expressed as:

$$\sigma = \frac{nZ^2e^2D}{K_BT} \qquad (2)$$

where σ = ionic conductivity $\left(\frac{S}{cm}\right)$
n = ion number density (ions/cm^3)
z= charge number of Li^+ (1)
e = elementary charge $(1.602\ x\ 10^{-19}\ C)$
D = diffusion coefficient (cm^2/s)
K_B = Boltzmann constant $(1.38x10^{-23}\ J/K)$
T = absolute temperature (K)

Typical D values for polymer electrolytes at room temperature are 10^{-12} to $10^{-9}\ cm^2/s$ (Zhang *et. al.,* 2019).

Fick's Law of Diffusion

Fick's first law of diffusion states that the diffusion flux is proportional to the negative gradient of concentration (Fong *et. al.,* 2021). It is given by:

$$J = -D\frac{dC}{dx} \qquad (3)$$

$$but\ \frac{dC}{dX} \approx \frac{C}{L}$$

where J = diffusion flux $(mol/m^2.s)$
D =diffusion coefficient (m^2/s)
$\frac{dC}{dX}$ =concentration gradient $(mol\ /\ m^4)$
C = concentration of lithium salt (mol/m^3)
L =thickness of electrolyte (m)

Typical theoretical values for diffusion flux at room temperature lie within 10^{-9}-$10^{-4}\ mol/m^2$(Zhang *et.al.,* 2022).

Faraday's Law of Electrolysis

Faraday's law of electrolysis, which states that the amount of substance deposited at an electrode during electrolysis is directly proportional to the quantity of electric charge passed through the electrolyte (Bard & Faulkner, 2021).

The Faraday's first law of electrolysis (Bard & Faulkner, 2021) is expressed as:

$$n = \frac{Q}{ZF} \qquad (4)$$

Therefore, $Q = n\,.\,Z.F$ (5)

$$Q = J.A.t.Z.F \qquad (6)$$

where
n = moles or amount of Li^+(mole)

Q = electric charge (coulombs)
Z =valence of Li^+ (+ 1)
F= Faraday's constant $(96,485\ C/mol)$
J = diffusion flux
A = electrode area (m^2)
t = model time $(1s)$
Typical electric charge values are within 10^{-8} to $10^{-4}C/s$ (Bard & Faulkner, 2021).

Stress-Strain Model
Stress-strain model describes how materials respond to mechanical loads through elastic or plastic deformation (Zhao *et. al.,* 2018). From this theory, the ultimate tensile strength and strain equation (Smith & Lee, 2021) is as follows:

$$\sigma max = \frac{Fmax}{A} \quad (7)$$

where σmax = ultimate tensile strength (N/mm2)
$Fmax$ =load at break (N)
A = cross-sectional area (mm^2)

$$\varepsilon = \frac{\triangle L}{Lo} \quad (8)$$

where ε = tensile strain
$\triangle L$ = extension at break or change in length
Lo = tensile strain gauge length or original length

Kissinger Model
Kissinger Model determines the activation energy (E_a) of a material's decomposition using TGA data (Song & Kwak, 2022). The Kissinger equation is as follows:
Kissinger equation:

$$\ln\left(\frac{\beta}{T_P^2}\right) = \ln\left(\frac{AR}{E_a}\right) - \frac{E_a}{R\,T_p} \quad (9)$$

Rearranged Kissinger equation becomes,

$$\frac{E_a}{R\,T_p} = \ln\left(\frac{AR}{E_a}\right) - \ln\left(\frac{\beta}{T_P^2}\right) \quad (10)$$

Where
β =heating rate (K/min)
T_p = peak temperature $(in\ kelvin)$
E_a = activation energy $(K\,J/mol)$
A = pre-exponential factor (s^{-1}) for polymer degradation is generally within the range of 10^{10} to 10^{13} s^{-1}. (Vyazovkin *et. al.,* 2011)
R = gas constant $(8.314J/mol.K)$
Vyazovkin (2019) gave the criterion for thermal stability as follows:

i. Low thermal stability (low activation energy): $<100KJ/mol$
ii. Moderate thermal stability (moderate activation energy): $100 - 200KJ/mol$
iii. High thermal stability (high activation energy): $>200KJ/mol$

Predictive Model
Multiple Regression Model
A multiple regression model is a predictive statistical technique used to evaluate the relationship between a dependent variable and several independent variables (Frost, 2019). In this study, the dependent variables are the theoretically analyzed values of ionic conductivity, ultimate tensile strength, and activation energy, while the independent variables are the varying mass ratios of cassava starch and PVP. The Multiple Regression model is as follows:

$$\bar{Y}_i = b_1 + b_2X_1 + b_3X_2 \quad (11)$$

where $\bar{Y}_i$ = predicted dependent variables
X_1= mass of cassava starch (g)
X_2 = mass of PVP (g)
b_1, b_2, b_3 = regression coefficients

MATERIALS AND METHODS

Materials
The materials used in this work consist of lithium acetate dihydrate $(LiOOCCH_3.2H_2O)$ (99%), polyvinylpyrrolidone (PVP) (98%), cassava starch powder (95%), titanium dioxide (TiO_2)(99%), borax (98%), glycerol (98%), and deionized water (99.9%). Cassava starch powder was locally prepared, while $LiOOCCH_3.2H_2O$, PVP, TiO_2, borax, glycerol and deionized water were purchased through a vendor at African University of Science and Technology, Galadima, FCT-Abuja.

Preparation of Cassava Starch Powder
Cassava starch powder was prepared based on Arrieta *et. al.* (2023) procedures. The procedures involved washing and peeling off the skin of a cassava tubers. The peeled tubers were then disintegrated by grinding using industrial grinding processor. The grinded tubers were then placed in deionized water, stirred for 15mins, and filtered through muslin cloth. The filtered liquid was left to settle down for 12 hrs., to allow it to precipitate. The precipitated starch was obtained after removing water left on top of it. The precipitated cassava starch was then washed three times with deionized water and dried in an oven for 24 hrs. at 50^0C. The dried precipitated cassava starch was then grinded using household electric grinding machine to obtain cassava starch powder.

Preparation of Nanocomposite Polymer Electrolyte Films
The nanocomposite polymer electrolyte films were prepared using direct heating solution casting method as illustrated by Isnugroho and Endarko (2018). The nanocomposite polymer electrolyte materials composition is presented on Table 1.

Table 1: Compositions of Cassava Starch-Polyvinylpyrrolidone Nanocomposite Polymer Electrolytes

Sample	CS (g)	PVP (g)	Glycerol (ml)	Borax (g)	Titanium Dioxide (g)	Lithium Acetate dihydrate (g)
S1	0	5	2	0.3	0.15	0.5
S2	1.5	3.5	2	0.3	0.15	0.5
S3	2.5	2.5	2	0.3	0.15	0.5
S4	3.5	1.5	2	0.3	0.15	0.5
S5	5	0	2	0.3	0.15	0.5

Based on the above composition, the PVP or CS solutions were prepared using 15-50mL of deionized water. The solution was heated at 60 ^{0}C for 30minutes and stirred using a magnetic stirrer at 750rpm. After 30 minutes, glycerol was added and mixed for another 10minutes. Subsequently, borax and TiO_2 were added and mixed for an additional 10 minutes. Finally, lithium acetate dihydrate was added and mixed with the solution for another 20 minutes. At end of 20 minutes, the solution was cast onto three Teflon sheets and dry at room temperature for 48hrs. The dried films were then peeled off from the Teflon sheets using a razor blade and used for experiment.

The preparation of Cassava Starch-Polyvinylpyrrolidone nanocomposite polymer electrolyte film using direct heating solution casting method is shown in Figure 1.

Figure 1: Preparation of Cassava Starch- Polyvinylpyrrolidone Nanocomposite Polymer Electrolyte

Electrochemical Impedance Spectroscopy Method

EIS (Gamry Reference 600) was used to record impedance spectra from 1Hz to 1MHz at 10mV AC amplitude, with films placed between stainless-steel blocking electrodes. Bulk resistance from Nyquist plots was used to compute ionic conductivity (Yan, 2020). Conductivity values were further analysed using the Nernst-Einstein model (Maier, 2004), Fick's law of diffusion (Fong *et. al.,* 2021), and Faraday's law of electrolysis (Bard & Faulkner, 2021).

Universal Testing Machine Method

UTM (Instron 3345) was used to record the tensile strength data. The recorded data are the imposed loads and the film extensions. The UTM also provided the load-extension plot, and other details such as the stain at break, extension at break and load at break. These data were analyzed using stress and strain models (Zhao *et. al.,* 2018) to derive the ultimate tensile strengths and strains of nanocomposite polymer electrolyte films.

Thermogravimetric Analysis

TGA (PerkinElmer TGA 4000) was used to record thermal stability data to 950^{0}C at a heating rate of 10^{o}C/min, producing weight-loss versus temperature plots. The Kissinger model was applied to TGA data to compute activation energy of thermal degradation, which is used to quantify thermal stability (Song & Kwak, 2022, Vyazovkin, 2019).

RESULTS AND DISCUSSION

Theoretical Models

Ionic Conductivity Model

The ionic conductivity of Sample 1-5 was examined using Nyquist plot and ionic conductivity equation, as presented in Figure 2(a-e) and Table 2.

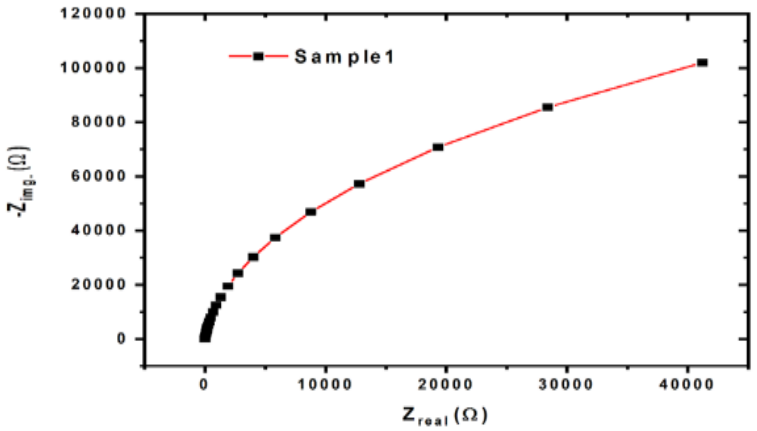

Figure 2a: Nyquist Plot of Sample 1

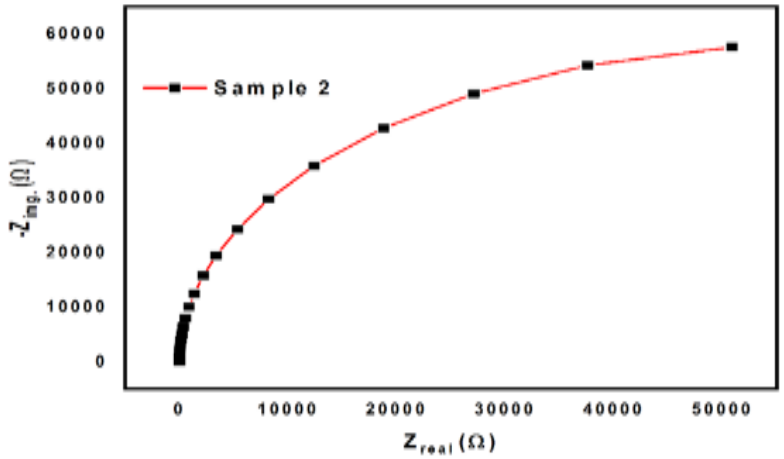

Figure 2b: Nyquist Plot of Sample 2

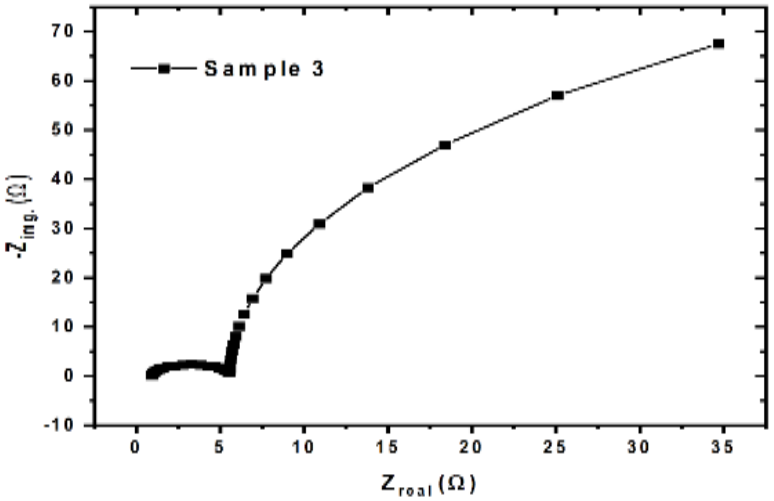

Figure 2c: Nyquist Plot of Sample 3

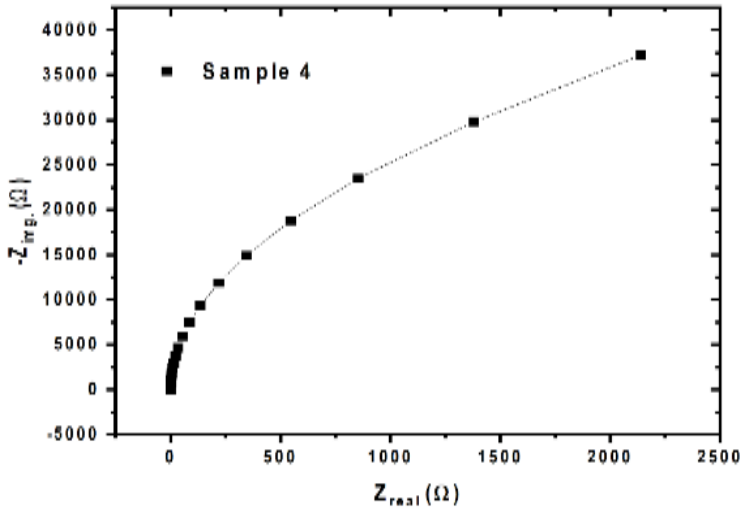

Figure 2d: Nyquist Plot of Sample 4

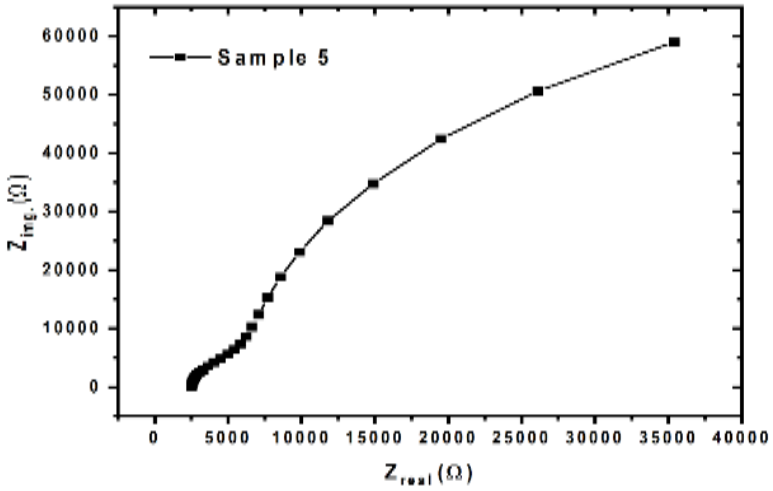

Figure 2e: Nyquist Plot of Sample 5

Table 2: Ionic Conductivities of Nanocomposite Polymer Electrolytes

Sample	Rb ($ohms$)	Thickness, (cm)	Diameter, D(cm)	Area, A (cm^2)	Ionic Conductivity, σ (s/ cm)
1	500	0.02	1.5	1.77	2.26 x 10^{-5}
2	1000	0.02	1.5	1.77	1.13 x 10^{-5}
3	6.5	0.02	1.5	1.77	1.74 x 10^{-3}
4	50	0.02	1.5	1.77	2.26 x 10^{-4}
5	6250	0.02	1.5	1.77	1.81 x 10^{-6}

Sample 3 recorded the highest ionic conductivity ($1.74x10-3\ s/cm$). This is consistent with optimal polymer chain mobility at a balanced CS-PVP ratio; while Sample 5 has the lowest ionic conductivity of 1.81x10^{-6}s/cm. However, all samples ionic conductivities fell within the typical ionic conductivities of 10^{-6} to 10^{-3}s/cm (Ramesh & Arof, 2021). This finding agrees with that Chu (2023), Gustav (2016) and Jing *et.al.* (2021), who reported an ionic conductivity that fall within the same range of 10^{-6} to 10^{-3}s/cm. However, the finding disagrees with that of Wijanarko *et.al.* (2024) who reported low ionic conductivity of 10^{-11}s/cm for corn starch polymer and lanthanum nitrate superconductor.

Nernst-Einstein Model

The ionic diffusion of Sample 1-5 was analysed using Nernst-Einstein model, as presented in Table 3.

Table 3: Ionic Diffusion Coefficients in Nanocomposite Polymer Electrolytes

Sample	σ (s/cm)	KB (J/K)	Temp. (K)	Num. Density, n ($ions/cm^3$)	Valence, z	Elem. Charge, C	Diffusion Coefficient D (cm^2/s)
1	$2.26x10^{-5}$	$1.38x10^{-23}$	298	$8.337x10^{22}$	1	$1.602x10^{-19}$	$4.34x10^{-11}$
2	$1.13x10^{-5}$	$1.38x10^{-23}$	298	$8.337x10^{22}$	1	$1.602x10^{-19}$	$2.17x10^{-11}$
3	$1.74x10^{-3}$	$1.38x10^{-23}$	298	$8.337x10^{22}$	1	$1.602x10^{-19}$	$3.34x10^{-9}$
4	$2.26x10^{-4}$	$1.38x10^{-23}$	298	$8.337x10^{22}$	1	$1.602x10^{-19}$	$4.34x10^{-10}$
5	$1.81x10^{-6}$	$1.38x10^{-23}$	298	$8.337x10^{22}$	1	$1.602x10^{-19}$	$3.48x10^{-12}$

The diffusion coefficient followed the same trend as ionic conductivity, with Sample 3 exhibiting the highest value ($3.34x10^{-9}$ cm^2/s); while Sample 5 has the lowest diffusion coefficient of $3.48x10^{-12}cm^2/s$. However, all samples diffusion coefficients fell within the typical diffusion coefficients ranges of 10^{-12} to $10^{-9}cm^2/s$ (Zhang *et. al.* 2019).

Fick's Law of Diffusion

The diffusion fluxes of Sample 1-5 were analysed using Fick's law of diffusion, as presented in Table 4.

Table 4: **Diffusion Fluxes in Nanocomposite Polymer Electrolytes**

Sample	Diffusion Coefficient, Dcm^2/s)	Concentration, c ($mol./m^3$)	Thickness, L(m)	Diffusion Flux, J ($mol./m^2.s$)
1	$4.34x10^{-11}$	$1.38x10^5$	0.0002	$2.995x10^{-6}$
2	$2.17x10^{-11}$	$1.38x10^5$	0.0002	$1.50x10^{-6}$
3	$3.34x10^{-9}$	$1.38x10^5$	0.0002	$2.31x10^{-4}$
4	$4.34x10^{-10}$	$1.38x10^5$	0.0002	$2.99x10^{-5}$
5	$3.48x10^{-12}$	$1.38x10^5$	0.0002	$2.40x10^{-7}$

Sample 3 again showed the highest diffusion flux ($2.31x10^{-4}$ mol/m^2s), while Sample 5 has the lowest diffusion flux of $2.40x10^{-7}mol/m^2s$. confirming its enhanced ion mobility relative to other compositions. All samples diffusion fluxes fell within the typical diffusion fluxes ranges of 10^{-9} to 10^{-4} mol/m^2s (Zhang *et. al.* 2022).

Faraday's Law of Electrolysis

The electric charges of Sample 1-5 were analysed using Faraday's law of electrolysis, as presented in Table 5.

Table 5: Electric Charges of Nanocomposite Polymer Electrolytes

Sample	Diffusion Flux, J($mol./m^2.s$)	Area (m^2)	Model Time (s)	Valence, z	Faraday's Constant (F)	Electric Charge, Q (C)
1	$2.995x10^{-6}$	0.000177	1	1	96,485	$5.11x10^{-5}$
2	$1.50x10^{-6}$	0.000177	1	1	96,485	$2.56x10^{-5}$
3	$2.31x10^{-4}$	0.000177	1	1	96,485	$3.94x10^{-3}$
4	$2.99x10^{-5}$	0.000177	1	1	96,485	$5.11x10^{-4}$
5	$2.40x10^{-7}$	0.000177	1	1	96,485	$4.1x10^{-6}$

Electric charge values followed the established trend, with Sample 3 yielding the highest ($3.94x10^{-3}C/s$), while Sample 5 has the lowest electric charge of $4.1x10^{-6}C/s$ All samples electric charges fell within the typical electric charges ranges of 10^{-8} to $10^{-4}C/s$ (Bard & Faulkner, 2021). This further showed that it is consistent with ionic conductivity, ionic diffusion and diffusion flux.

Stress and Strain Model

The ultimate tensile strength and strain parameters of Sample 1-5 was analysed using Stress and Strain model, as presented in Table 6.

Table 6: Ultimate Tensile Strengths and Strains of Nanocomposite Polymer Electrolytes

Sample	Gauge Length (mm)	Cross Sectional Area (mm^2)	Load at Break (N)	Extension at Break (mm)	Strain or Elongation (%)	Ultimate Tensile Strength(N/mm^2)
1	50	0.8	0.471	27.628	55.25	0.589
2	50	0.8	0.0646	14.191	28.38	0.081
3	50	0.8	-1.668	18.610	37.22	-2.085
4	50	0.8	-0.037	8.023	16.05	-0.046
5	50	0.8	-0.646	14.535	29.07	-0.808

All samples exhibited low ultimate tensile strength, which may be due to its soft condensed nature; however, in terms of flexibility, Sample 1 exhibited the highest strain (55.25%); which was followed by Sample 3 having a strain of 37.22%. These results align with the findings of Chu (2023), who reported that higher tensile strain is associated with polymer content. However, the findings contrast with Raut *et.al.* (2019), who observed that composite solid polymer electrolytes can exhibit tensile strength values up to 6 times higher than those of pure solid polymer electrolytes.

Kissinger Model

The activation energies of Sample 1-5 were analyzed using Kissinger model, as presented in Figure 3(a-e) and Table 7.

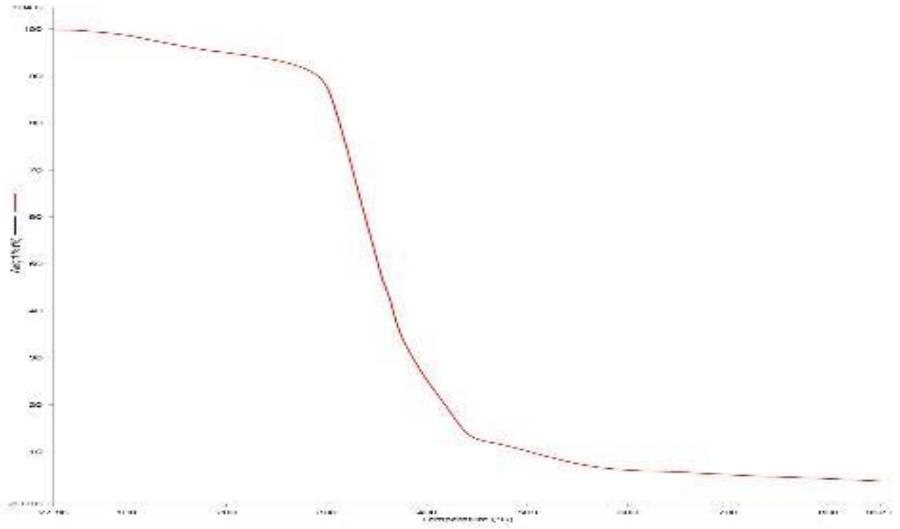

Figure 3a: Thermogravimetric Curve of Sample 1

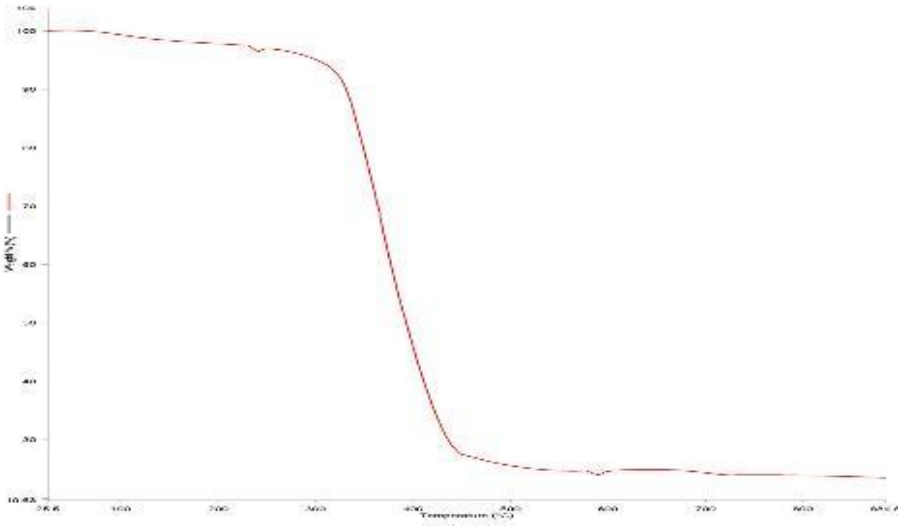

Figure 3b: Thermogravimetric Curve of Sample 2

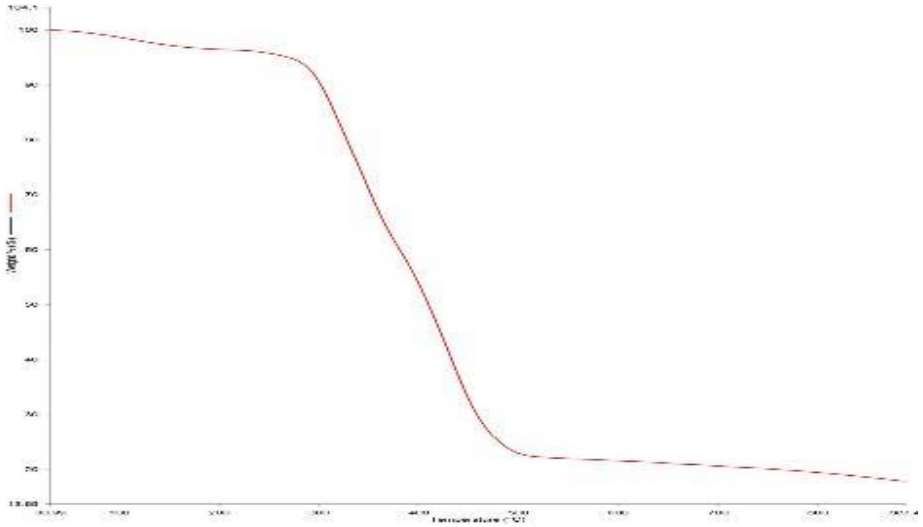

Figure 3c: Thermogravimetric Curve of Sample 3

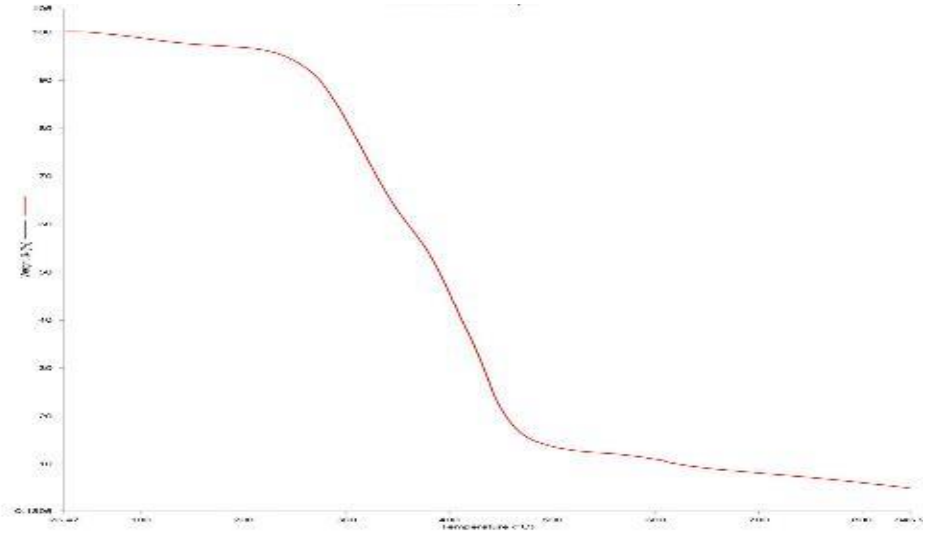

Figure 3d: Thermogravimetric Curve of Sample 4

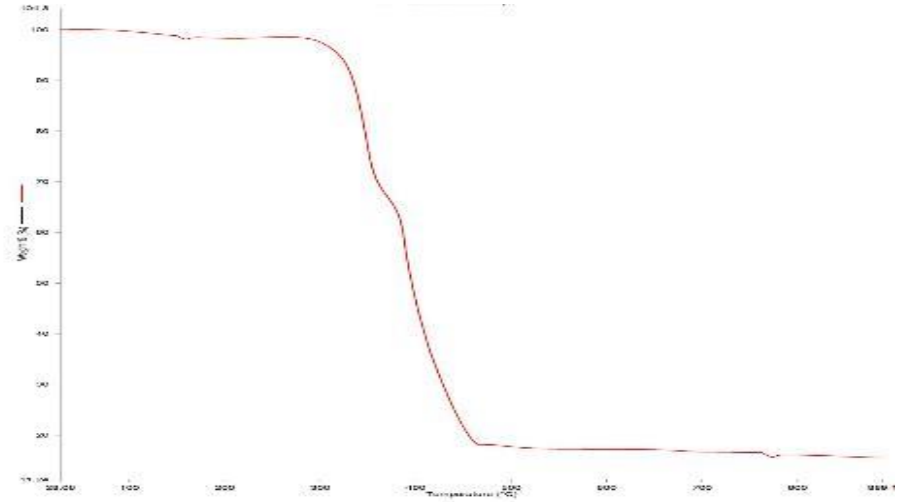

Figure 3e: Thermogravimetric Curve of Sample 5

Table 7: Activation Energies of Nanocomposite Polymer Electrolytes

Sample	Heating Rate, β (K/s)	Peak Temperature, Tp (K)	Pre-Exponential Factor, A (s^{-1})	Gas Constant, R (Kj/mol.K)	Activation Energy, Ea(KJ/mol)
1	0.1667	623.15	10^{13}	$8.314x10^{-3}$	179
2	0.1667	643.15	10^{13}	$8.314x10^{-3}$	185
3	0.1667	653.15	10^{13}	$8.314x10^{-3}$	188
4	0.1667	658.15	10^{13}	$8.314x10^{-3}$	189
5	0.1667	673.15	10^{13}	$8.314x10^{-3}$	194

Sample 5 recorded the highest activation energy of 194KJ/mol; while other samples including sample 5 activation energies fall within the moderate thermal stability of 100-200KJ/mol, as stated by Vyazovkin (2019). These results are consistent with the findings of Andersson *et.al.* (2022), Tsurumaki *et.al.* (2022), Gustav (2016), Arrieta *et.al.* (2024) and Slesanrenko *et. al.* (2023) who reported that polymer electrolytes exhibited moderate thermal stabilities above 100^0C. However, the result is in contrast with the findings of Arrieta *et.al.* (2023) and Raut *et. al.* (2019), who reported thermal stability of polymer electrolytes to be below 100^0C.

Predictive Model

Multiple Regression Model

The predicted performance parameters determined using multiple regression models and their coefficient of determination (R^2) are presented in Tables 8 (a-c) and 9 respectively.

Table 8a: Predicted Ionic Conductivity Result using Multiple Regression Model

Sample	Y_i (Observed Ionic Conductivities) (s/cm)	X_1 (CS) (g)	X_2 (PVP) (g)	$\hat{Y}_i$ (Predicted Ionic Conductivities) (s/cm)
1	$2.26x10^{-5}$	0	5	$3.72x10^{-4}$
2	$1.13x10^{-5}$	1.5	3.5	$3.89x10^{-4}$
3	$1.74x10^{-3}$	2.5	2.5	$4.00x10^{-4}$
4	$2.26x10^{-4}$	3.5	1.5	$4.12x10^{-4}$
5	$1.81x10^{-6}$	5	0	$4.28x10^{-4}$

Table 8b: Predicted Tensile Strength Result using Multiple Regression Model

Sample	Y_i (Observed Ultimate Tensile Strength) (N/mm^2)	X_1 (CS) (g)	X_2 (PVP) (g)	$\hat{Y}_i$ (Predicted Ultimate Tensile Strength) (N/mm^2)
1	0.589	0	5	0.170
2	0.081	1.5	3.5	-0.204
3	-2.085	2.5	2.5	-0.454
4	-0.046	3.5	1.5	-0.703
5	-0.808	5	0	-1.078

Table 8c: Predicted Activated Energy Result using Multiple Regression Model

Sample	Y_i (Observed Activated Energy) (KJ/mol)	X_1 (CS) (g)	X_2 (PVP) (g)	$\hat{Y}_i$ (Predicted Activated Energy) (KJ/mol)
1	179	0	5	180
2	185	1.5	3.5	184
3	188	2.5	2.5	187
4	189	3.5	1.5	190
5	194	5	0	194

Table 9: Multiple Regression Coefficient and Validation Parameters

Performance Parameters	Regression Coefficients			Validation Parameters		
	b1	b2	b3	RMSE	MAE	R^2
Ionic Conductivity	$2.97x10^{-5}$	$7.97x10^{-5}$	$6.85x10^{-5}$	$6.75x10^{-4}$	$5.36x10^{-4}$	$8.02x10^{-4}$
Ultimate Tensile Strength	-0.034	-0.21	0.041	0.83	0.65	0.21
Activation Energy	-96.47	58.12	55.26	0.80	0.75	0.97

The multiple regression analysis of predicted ionic conductivity and ultimate tensile strength using CS and PVP as independent variables, The multiple regression analysis revealed a low coefficients of determination of $R^2 = 8.02x10^{-4}$ and $R^2= 0.21$, for ionic conductivity and ultimate tensile strength respectively, indicating their unsuitability for prediction purposes. In contrast, the activation energy model showed a strong predictive performance ($R^2= 0.97$).

CONCLUSION

The particle dynamics in nanocomposite polymer electrolytes was analysed using theoretical and predictive models. The findings on ion transport revealed that Sample 3, with an equal blend proportion of CS and PVP produces a nanocomposite polymer electrolyte that has the highest ionic conductivity ($1.74x10^{-3}$ s/cm), highest ionic diffusion coefficient ($3.34x10^{-9}cm^2/s$), highest diffusion flux ($2.31x10^{-4}mol/m^2.s$), and highest electric charge ($3.94x10^{-3}C/s$).

Findings on ultimate tensile strength showed a general low strength due to the soft nature of polymer electrolytes, however, Sample 1 recorded the highest strain (55.25%); followed by Sample 3 having a strain of 37.22%. All the samples activation energies fell within moderate thermal stability of 100-200KJ/mol, with Sample 5 exhibiting the highest activation energy of 194KJ/mol. Result on predictive model indicated that only the activation energy result had a strong predictive performance ($R^2= 0.97$).

Based on these findings, it is recommended that Sample 3 nanocomposite polymer electrolyte with equal CS:PVP ratios be considered for industrial-scale applications due to their outstanding electrical properties, including high ionic conductivity, diffusion coefficient, diffusion flux and electric charge.

REFERENCES

Andersson, R., Hernandez, G., See, J., Flaim, T.D., Brandell, D., & Mindemark, J. (2022). Designing polyurethane solid polymer electrolytes for high temperature lithium metal batteries. *ACS Appl. Energy Mater, 2022, 5, 407-418.* https://doi.org/10.1021/acsaem.1c02942.

Armand, M., & Tarascon, J.M. (2008). Building better batteries. *Nature, 451, 7159, 652-657.* https://doi.org/10.1038/451652a.

Arrieta, A.A., Calabokis, O.P., & Mendoza, J.M. (2023). Effect of lithium salts on the properties of cassava starch on solid biopolymer electrolytes. *Polymers 2023, 15, 20, 1-3. Doi:10.3390/polym1520450.*

Arrieta, A.A., Calabokis, O.P., & Vanegas, C. (2024). Influence of lithium triflate salt concentration on structural, thermal, electrochemical, and ionic conductivity properties of cassava state solid biopolymer electrolytes. *Int. J. Mol. Sci 25, 15, 8450,* https://doi.org/10.3390/ijms25158450.

Bard, A.J., & Faulkner, L.R. (2021). *Electro-chemical methods: Fundamentals and Applications* (2nd ed.). Wiley

Barde, F., & Deschamps, M. (2015). Nernst-Einstein relation and ionic conductivity in polymer electrolytes. *The Journal of Chemical Physics, 143, 24, 244904.* https://doi.org/10.1063/1.4938398.

Cabaret, D.M., Grandou, T., Grange, G.M., & Perrier, E. (2022). Elementary particles: What are they? substances, elements, and primary matter. *Foundations of Science, 27, 2, 722-753.* https://doi.org/10.1007/s10699-021-09826.

Callister, W.D., & Rethwisch, D.G. (2020). *Materials science and engineering: An introduction* (10th ed.). Wiley.

Chu, H.J. (2023). Potential composite solid-state electrolyte for lithium-ion battery. *A published MSc thesis in Material Science and Engineering from University of California.*

Fong, K.D., Self, J., McCloskey, B.D., & Persson, K.A. (2021). Ion correlations and their impact on transport in polymer-based electrolytes. *Macromolecules, 54, 6, 2575-2591.* https://doi.org/10.1021/acs.macromol.OcO25.

Frost, J. (2019). Regression analysis: An intuitive guide for using and interpreting linear models. *Journal of Statistics Education, 27, 2, 130-140.* https://doi.org/10.1080/10691898.2019.1597077.

Griffiths, D.J. (2008). *Introduction to elementary particles* (2nd ed.). Wiley.

Gustav, E. (2016). A study of poly (vinyl alcohol) as a solid polymer electrolyte for lithium ion batteries. *UPPSALA UNIVERSITET,* http://www.teknat.uu.se/student.

Isnugroho, D., & Endarko, E. (2018). Preparation and characterization of cassava starch-based polymer electrolyte membrane doped with lithium perchlorate. *AIP Conference Proceedings, 2023, 020034.* https://doi.org/10.1063/1.5064123

Jing, B., Wang, X., Shi, Y., Gao, H., & Fullerton-Shirey, S.K. (2021). Combining hyperbranched and linear

structures in solid polymer electrolytes to enhance structures in solid polymer electrolytes to enhance mechanical properties and room-temperature ion transport. *Front.Chem.9: 563864.* https://doi.org/10.3389/Fchem.2021.563864.

Kittel, C. (2005). *Introduction to solid state physics (8th ed.).* Wiley.

Lasia, A. (2014). *Electrochemical Impedance Spectroscopy and its Applications*. Springer. https://doi.org/10.1007/978-1-4614-8933-7.

Macdonald, J.R., & Barsoukov, E. (2005). *Impedance Spectroscopy: Theory, Experiment and Applications* (2nd ed.). Wiley-Interscience.

Maier, J. (2004). *Physical chemistry of ionic materials: Ions and electrons in solid*. Wiley.

Nagaura, T., & Tozawa, K. (1990). Lithium ion rechargeable battery. *Progress in Battery and Battery Materials, 9, 2, 3-9.*

Patel, K. (2021). *Ionic transport and mechanical stability in nanocomposite polymer electrolytes.* CRC Press.

Pathak, T.S., Yun, J.H., Lee, W.J., & Lee, Y.S. (2014). Green and sustainable solutions for development of bio-based polycarbonate from isosorbide: *A review. Journal of Cleaner Production, 77, 85-96.* https://doi.org/10.1016/j.jclepro.2013.12.031.

Patra, N., Ramesh, P., Donthu, V., & Ahmad, A. (2024). Biopolymer-based composites for sustainable energy storage: Recent developments and, future outlook. *Journal of Materials Sciences: Materials on Engineering, 19, 34.* https://doi.org/10.1186/s40712-024-00181-9.

Raihan, R., Fairuzdzah, A.L., Asiah, M.N., & AbMalik, M.A. (2022). The compatibility of jackfruit seed starch and polyvinyl alcohol blend as biopolymer electrolyte host. *Malaysian Journal of Analytical Sciences, 26, 4, 829-837.*

Ramesh, S., & Arof, A.K. (2021). Investigation of electrical and electrochemical properties of poly(vinyl chloride) -based polymer electrolytes. *Solid State Ionics, 140, 3-4, 291-298.* https://doi.org/10.1016/s0167-2738(01)00718-1.

Raut, P., Li, S., Chen, Y., Zhu, Y., & Jana, S.C. (2019). Strong and flexible composite soli polymer electrolyte. Membranes for Li-ion batteries. *ACS Omega, 4, 18203-18209.*

Slesarenko, N.A., Chernyak, A.V., Khatmullina, K.G., Baymuratova, G.R., Yudina, A.V., Tulibaeva, G.Z., Shestakov, A.F., Volkov, V.I., & Yarmolenko, O.V. (2023). Nanocomposite polymer gel electrolyte based on TiO_2 nanoparticles for lithium batteries. *Membranes, 13, 776.* https://doi.org/10.2290/membranes13090776.

Smith, J.D., & Lee, R.T. (2021). Evaluating the mechanical properties of polymer composites using universal testing machines. *Journal of Materials Science and Engineering, 45, 3, 123-130.* https://doi.org/10.1016/j.jmse.2021.03.015.

Song, M. Y., & Kwak, Y.J. (2022). Determination of the activation energy for hydride decomposition using a Sieverts-Type Apparatus and the Kissinger Equation. *Metals, 12, 2, 265.* https://doi.org/10.3390/met12020265.

Tsurumaki, A., Rettaroli, R., Mazzapioda, L., & Navaira, M.A. (2022). Inorganic-organic hybrid electrolytes based on AI-doped $Li_7La_3Zr_2O_{12}$ and ionic liquids. *Appl. Sci. 2022, 12, 7318.* https://doi.org/10.3390/app12147318.

Wang, H., Xu, Y., Zhang, Y., & Song, Y. (2019). Thermogravimetric analysis and thermal stability of polymer electrolytes for lithium batteries. *Journal of Thermal Analysis and Calorimetry, 135, 175-185.* https://doi.org/10.1007/s10973-018-7029-9.

Vyazovkin, S. (2019). Activation energy in thermal degradation of polymers. *Thermochimica Acta, 689, 178-184.*

Vyazovkin, S., Burnham, A.K., Criado, J.M., Perez-Maqueda, L.A., Popescu., C., & Sbirrazzuoli, N. (2011). ICTAC kinetics Committee recommendations for performing kinetic computations on thermal analysis data. *Thermochimica Acta, 520, 1-2, 1-19.* https://doi.org/10.1016/j.tca.2011.03.034.

Wijanarko, N.P., Wulandari, D., Arrafii, M.H., Pradanawati, S.A., Nimah, Y.L., Noerochim, L., & Hamidah, N.L. (2024). Effect of solid polymer electrolyte based on corn starch and lanthanum nitrate on the electrochemical performance of supercapacitor. *Bio Web of Conferences, 89, 03001.* https://doi.org/10.1051/biocontf/20248903001.

Yan, G. (2020). Mechanical behaviour of solid electrolyte materials for lithium-ion battery. *Energie & Unwett/Energy & Environment Band, 500.*

Zhang, X., Wang, C., Appleby, A.J., & Little, F.E. (2022). Characteristics of lithium-ion conducting

composite polymer-glass secondary cell electrolytes. *Journal of Power Sources, 112, 209-215.*

Zhang, H., Zhang, H., & Yao, X. (2019). Transport and electrochemical properties of PEO-based polymer electrolytes with lithium salt. *Solid State Ionics, 180, 26-27, 1434-1439.* https://doi.org/10.1016/j.ssi.2009.09.006.

Zhao, Q., Stalin, S., Zhao, C.Z., & Archer, L.A. (2018). Designing solid-state electrolytes for safe, energy-dense batteries. *Nature Reviews Materials, 5, 229-252.* https://doi.org/10.1038/s41578-020-0180-3.